

# Turbulence - minimum dissipation and maximum macroscopic momentum exchange

**Hans Paul Drescher**

Galileo-Allee 8, D-52457 Aldenhoven, Germany

[hanspaul.drescher@budi.de](mailto:hanspaul.drescher@budi.de)

Mai 2021

## **Abstract**

The minimum dissipation requirement of the thermodynamics of irreversible processes is applied to characterize the existence of laminar and non-laminar, and the co-existence of laminar and turbulent flow zones. Local limitations of the different zones and three different forms of transition are defined. For the Couette flow a non-local “corpuscular” flow mechanism explains the logarithmic law-of-the-wall, maximum turbulent dimensions and a value  $\chi = 0,415$  for the v. Kármán constant. Limitations of the logarithmic law near the wall and in the centre of the experiment are interpreted.

## **Keywords:**

Minimum dissipation condition, non-local flow mechanism, Kármán constant

## Table of Contents

	Page
<b>1. Introduction</b>	3
1.1 Fluid flow experiment, an irreversible process	3
1.2 The minimum dissipation requirement	3
1.3 Local and non-local flow forms, transition	5
<b>2. Couette flow</b>	6
<b>3. Three types of transition</b>	11
3.1 The continuous near-wall transition	11
3.2 The complete transition turbulent-to-laminar	12
3.3 The “forced” changeover laminar-to-turbulent	16
3.4 Results and consequences	19
<b>4. General conditions for turbulence, “<math>\mu_{\text{turb}} \geq 27 \mu</math>”</b>	21
<b>5. Limitations of the logarithmic “law-of-the-wall”</b>	23
<b>6. An analytical model: non-local character, logarithmic flow profile, v. Kármán constant, Prandtl’s mixing length</b>	25
<b>7. Numerical calculations</b>	33
7.1 A 1-dimensional equation for a turbulent profile	33
7.2 Numerical examples for Couette and pipe flow	35
<b>8. Summary</b>	39
<b>9. Acknowledgments</b>	41

Literature, Special parameters, Data Availability Statement

# **1. Introduction**

## **1.1 Fluid flow experiment, an irreversible process**

Distinguishing reversible and irreversible processes is a significant element of thermodynamics. Non-equilibrium, irreversible processes require a minimum condition for the production of entropy. I. Prigogine detailed that in his Nobel-lecture 1978 in Stockholm /1/.

We apply that statement to distinguish laminar and turbulent flow. Any flow experiment in the laboratory starts with minimum (or zero) flow speed. That situation, near (or at) an equilibrium, can be described by a laminar flow mechanism. Any turbulent experiment requires significant higher flow speeds, requiring a higher input of energy, accompanied by higher dissipation rates. Without an increase of external energy input the transition laminar-to-turbulent does not exist.

The Chapters 3.1 – 3.4 describe three different types of transition and the resulting consequences.

## **1.2 The minimum dissipation requirement**

The theorem of minimum entropy production of the thermodynamics of irreversible processes states that non-equilibration thermodynamic processes proceed in a manner in which the entropy production/dissipation becomes minimal /1/.

The theory of irreversible thermodynamic processes is associated with the names of Onsager (Nobel Prize 1966), Casimir, Eckart, Meixner, de Groot, and Prigogine (Nobel Prize 1977). The minimum requirement is mentioned as “Prigogine-Prinzip” in the German Brockhaus Enzyklopädie /2/ and as the “Rayleigh-Onsager principle of least dissipation or principle of minimum entropy production” in the British Encyclopaedia Britannica /3/.

In fluid dynamics theory the minimum principle has not always been accepted. Malkus and Busse /6/ concluded that dissipation is maximum in turbulent flow conditions: “The realized turbulent shear flow represents the flow with maximum dissipation at a given Reynolds number among all possible solutions of the Navier-Stokes equations.” This statement fully contradicts the theorems above and later results. Klimontovich /7/ verified the minimum condition for turbulence, his consequence is interesting but not complete.

The dissipation minimum has not only to be discussed for the total integrated dissipation of the experiment, but also for the local minimum at different flow positions. For turbulence the statements of Malkus/Busse /6/ postulate a general maximum dissipation, the statement of Klimontovich /4/ a general minimum dissipation. Both statements do not comply.

The physical principle of minimum entropy production/dissipation is not to be disputed. Every flow experiment is a dissipative, non-equilibrium process requiring a continuous input of mechanical energy, balanced by a corresponding dissipation rate. Any change or transition can be identified by a change of the dissipation rate.

There is a unique and important feature of the turbulent Couette flow, the shear stress  $\tau$  is constant along the turbulent flow profile

$$\tau = \text{const.} \quad (1)$$

but the dissipation  $\dot{E}$  is not. With  $\dot{E} \sim \tau \cdot \frac{du}{dy}$  (2)

a resulting logarithmic turbulent flow profile leads to a gradient and a dissipation becoming continuously lower with greater wall distance. The logarithmic flow profile depends on a non-local turbulent mechanism, describing the transport of mechanical energy input from the wall to the locus of dissipation inside the flow. Any form of transition can be identified by the dissipation rate.

In a steady state experiment the established laminar and turbulent flow zones are stable, characterized by the minimum dissipation condition.

The calculated dissipation rates in the following chapters identify three completely different forms of transition. The results show that a laminar solution does not exist above a special dimensionless wall distance  $y^+$  and a turbulent solution does not exist below another  $y^+$  value.

### 1.3 Local and non-local flow forms, transition

The minimum dissipation requirement does not model the different flow mechanisms. It characterizes their limits and restrictions by the important thermodynamic parameter – the entropy production/dissipation.

A rough distinction of local/non-local character can be used for laminar/turbulent flow forms. It is evident that the behaviour of a local position in a laminar flow can be described by local parameters like velocity, gradient, shear stress, dissipation. That is completely different in a turbulent flow. Especially the dissipation depends on non-local parameters at varying distance.

Interesting in that context is the transition. It is scarcely conceivable that a transition with a significant change of parameters is governed by an identical flow mechanism, which can be described by an identical fluid dynamics model. The turbulent zone with the logarithmic law of the wall is governed by the non-local parameter “wall distance”, but not by the viscosity  $\mu$ . The near-wall laminar zone is mainly influenced by the local parameter “viscosity”. The shear stress is constant for both.

Further flow mechanisms are to be considered. The thermodynamics of irreversible processes are not restricted to special physical descriptions. A fluid can also be considered as a system of discrete mass points (Prandtl's mixing lengths hypothesis, kinetic gas theory, Lattice-Boltzmann method), and its mechanical behaviour can be addressed by methods of the mechanics of point systems. Classical, theoretical mechanics describe extreme minimum properties of mechanical point systems. (1747 Maupertuis “Prinzip der kleinsten Wirkung”, later justified by Euler, Lagrange and Hamilton, 1829 Gauss, 1842 Jacobi “Prinzip des kleinsten Zwanges” /4/ /5/). Such models lead to a non-local description of fluid flow.

In Chapter 2 the Couette flow is described as an example. As a result three different fluid forms are identified and described as laminar, turbulent and “transition form”. The third flow form is not known in detail, but it is evident that it is different. Especially the dissipation rate has to be lower than in the laminar zone and higher than in the turbulent zone.

## 2. Couette flow

For fluid flow between parallel walls, Couette flow, the Navier-Stokes equations give a simple, one-dimensional, linear, stationary velocity profile /8/. Fig. 1 shows different turbulent flow profiles for  $Re = 2900$  and  $34000$ . Very important and unique to Couette flow, there is a constant shear stress along the complete flow profile, which can be laminar, turbulent or both.

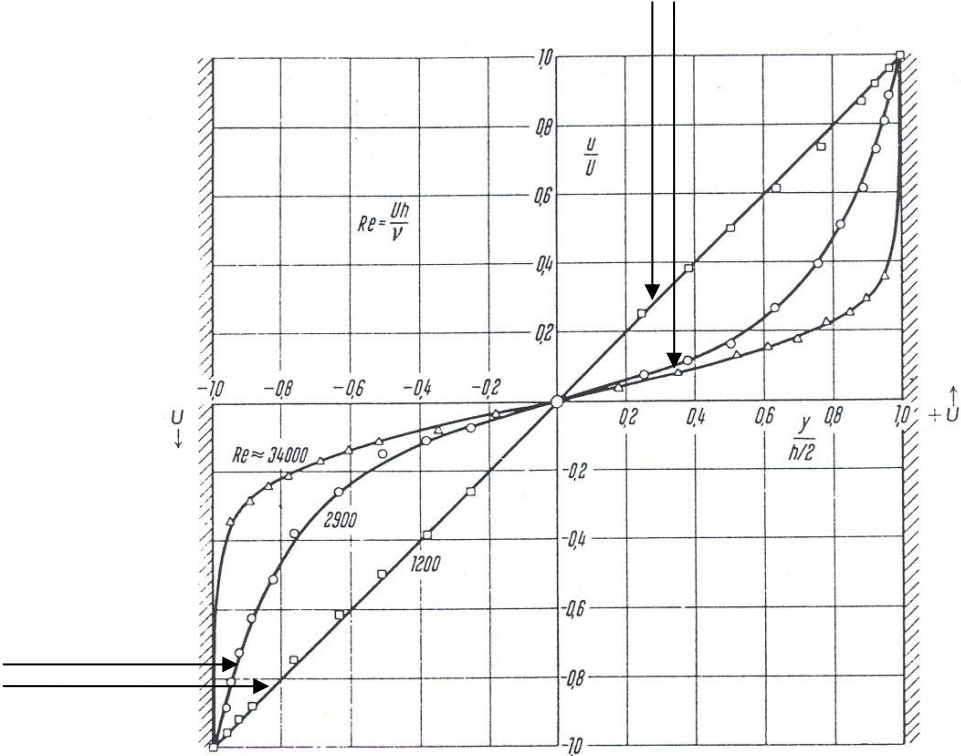


Fig. 1: Velocity profiles of Couette flow /8/

One can simplify the Couette flow profile into three zones, shown in Fig. 2.

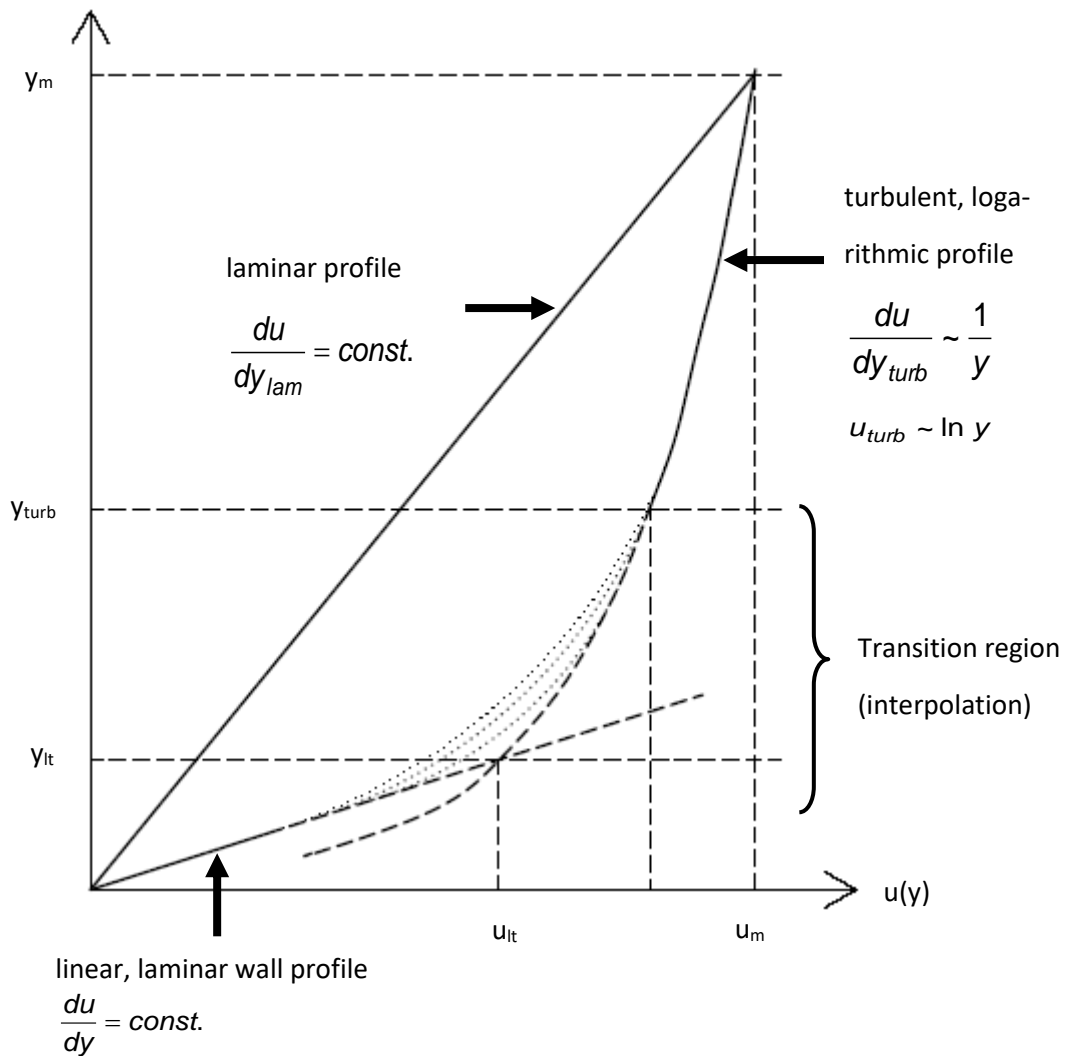


Fig. 2: Model assumption for the Couette flow

Zone 1: The turbulent zone, logarithmic flow profile

Zone 2: The transition zone

Zone 3: The linear (laminar) near-wall-zone

The description of zone 1 can be based on the “universal law of the wall” which is based on Prandtl’s and v. Kármán’s hypotheses /8/ with

$$\tau = \rho \chi^2 y^2 \left( \frac{du}{dy} \right)^2 \quad (3)$$

with  $\chi \approx 0,4$ , (v. Kármán constant)

Fig. 3, Fig. 4 show the theoretical formula and the empirical data for the logarithmic flow profile, given by Schlichting /8/ and Durst /9/ for low and high Re-numbers and wall distances.

The resulting logarithmic flow profile is fitted with experimental data to

$$\varphi(\eta) = 2.5 \ln \eta + 5,5 \quad /8/ \quad (4a)$$

or 
$$\varphi(\eta) = 2,47 \ln \eta + 5,17 \quad /9/ \quad (4b)$$

with

$$\varphi = u^+ = \frac{u}{\sqrt{\frac{\tau_0}{\rho}}} \quad (5)$$

as dimensionless so-called shear stress speed and

$$\eta = y^+ = \frac{y \cdot \sqrt{\frac{\tau_0}{\rho}}}{\frac{\mu}{\rho}} \quad (6)$$

as dimensionless wall distance /8/.

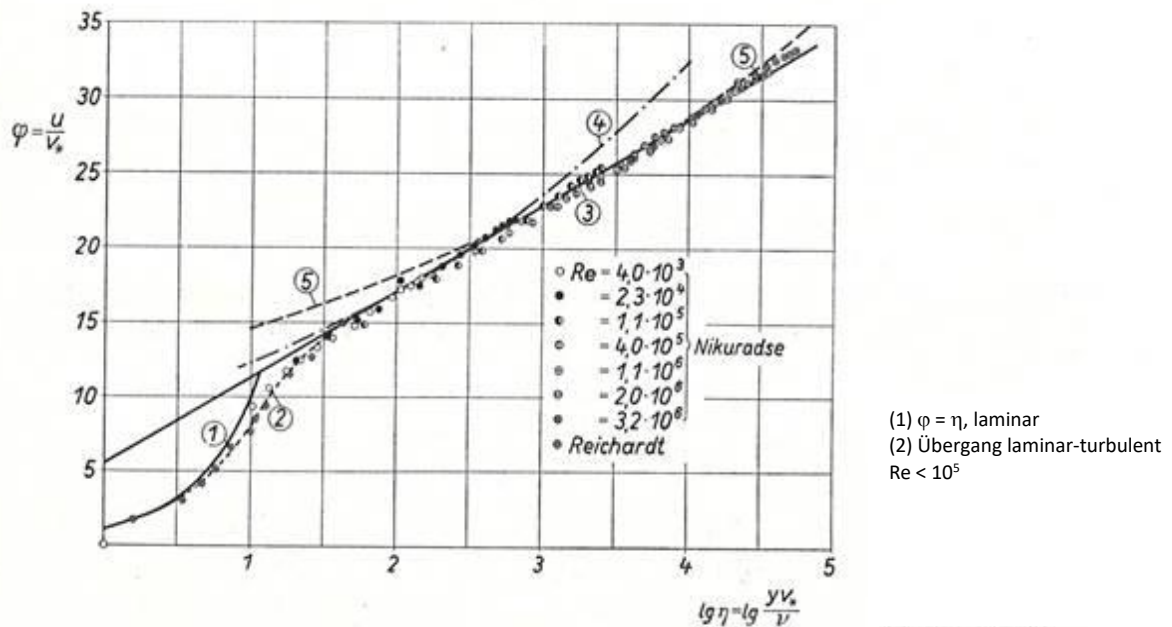


Fig. 3: Universal logarithmic velocity profile (law-of-the-wall)  $Re < 10^6$ , Schlichting /8/

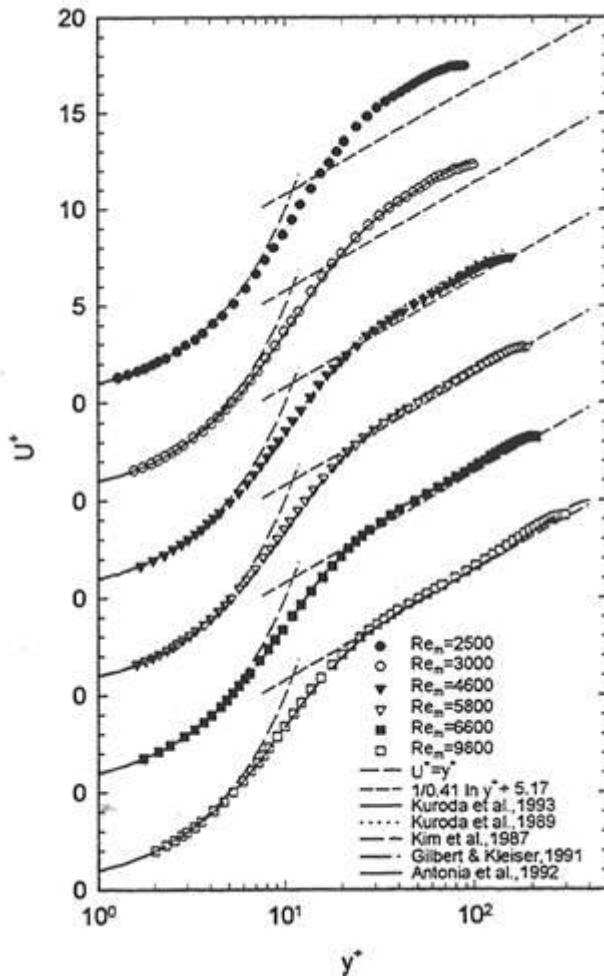


Fig. 4: Universal logarithmic velocity profile (law-of-the-wall) laser-doppler measurements,  $Re < 10^4$ , Durst /9/

The focus of the paper is the transition, thereby the limits of the validity of the “law of the wall”. Below the dimensionless wall distance  $y^+ \approx 50$  the logarithmic flow profile does not comply with experimental results. That is not surprising. The logarithmic law Eq. 4a, 4b is based on the constant shear stress  $\tau$  according Eq. 3. The integration to the final logarithmic formula includes integration constants which are fitted to the experiment /8/. At a wall distance  $y^+ = 0$  on the wall  $\varphi = -\infty$ . Consequently, Eq. 4a, b cannot be extrapolated near to the wall.

### Zone 3:

The viscous sublayer (and the linear profile of the laminar Couette flow) can be described by the Newton-Stokes friction within the Navier-Stokes equations.

$$\tau = \mu \cdot \frac{du}{dy} \quad (5)$$

exactly

$$\tau_{ij} = \mu \left( \frac{\partial u_j}{\partial x_i} + \frac{\partial u_i}{\partial x_j} \right) \quad (5a)$$

The linear near-wall profile is presented in Fig. 3, Fig. 4 in the simple (but curved) dimensionless form  $u^+ = y^+$ . Fig. 3, Fig. 4 show that the linear Newton-Stokes friction does not describe experimental results above  $y^+ \approx 11$ .

Zone 2:

For the transition zone we have little information. Reliable experimental data exist but no theoretical model.

The unique character of the Couette flow gives a marginal information. The shear stress  $\tau = \text{const.}$  along the Couette profile and the dissipation rate  $\dot{E}$  is

$$\dot{E} = \tau \cdot \frac{du}{dy}$$

With  $\frac{du}{dy}$  decreasing the dissipation becomes lower with greater wall distance.

That monotonously decreasing character of the dissipation is mandatory for a steady-state turbulent profile complying with the minimum dissipation requirement. On the other hand the dissipation, being constant very near the wall, is mandatory for a stable linear Navier-Stokes profile near the wall.

### 3. Three types of transition

#### 3.1 The continuous near-wall transition

The minimum dissipation requirement is applied to calculate the dimensionless thickness of the linear viscous sublayer near the wall of a turbulent Couette flow experiment. Fig. 2 shows basic model assumptions for the turbulent Couette experiment.

The linear profile near the wall in the viscous sublayer is calculated with the Navier-Stokes equations. The profile of the turbulent zone is calculated by the empirical logarithmic equation 4a.

Near the wall we assume

$$\frac{du}{dy}(y=0) = f \cdot \frac{u_m}{y_m} \quad (6)$$

with an unknown factor  $f$ .

The linear layer near the wall is defined by a lower dissipation compared to the turbulent dissipation rate at a greater wall distance  $y$ . With Eq. 2, Eq. 3, Eq. 6 follows

$$\rho \cdot \chi^2 y^2 \left(\frac{du}{dy}\right)^3 > \mu \cdot f^2 \left(\frac{u_m}{y_m}\right)^2 \quad (7)$$

For the Couette flow the shear stress over the profile, being laminar or turbulent, is constant

$$\rho \cdot \chi^2 y^2 \left(\frac{du}{dy}\right)^2 = \mu \cdot f \frac{u_m}{y_m} \quad (8)$$

Introducing Eq. 8 into Eq. 7 leads to

$$\rho \cdot \chi^2 y^2 \left(\frac{du}{dy}\right)^3 > \chi^4 \left(\frac{\rho}{\mu}\right)^2 y^4 \cdot \left(\frac{du}{dy}\right)^4 \cdot \mu \quad (9)$$

In Eq. 9 the factor  $f$  disappears. This leads to

$$\mu > \rho \cdot \chi^2 y^2 \frac{du}{dy} \quad (10)$$

and

$$\frac{1}{\chi^2} > \frac{y^2 \frac{du}{dy}}{\frac{\mu}{\rho}} \quad (11)$$

We introduce the dimensionless wall distance  $y^+ = \frac{y \cdot u_x}{\frac{\mu}{\rho}}$  /8/ with the so-called shear stress

$$\text{speed } u_x = \sqrt{\frac{\tau}{\rho}}$$

With  $\tau = \mu \frac{du}{dy}(0) = \text{const.}$  Eq. (11) becomes

$$\frac{1}{\chi} > y^+$$

or

$$y^+ \leq 2,5 \quad (12)$$

Schlichting /8/ describes experimental values with  $y^+ = 5$ , a calculation by Drescher /10/ gives  $y^+ = 3,4$ . There are experimental results near the wall by Durst /11/, with a linear flow profile below  $y^+ \leq 2$ .

We should be careful with the interpretation of Eq. 12. We do not know details of the mechanism of the transition zone. Due to the constant shear stress of the Couette flow we only know that the gradient of the transition zone has to be lower than that of the viscous sublayer and higher than that of the turbulent zone. Therefore, we interpret the value in Eq. 12 in a manner that it is the upper limit for the dimensionless thickness of the linear sublayer.

The situation at the limit of the linear viscous sublayer is stable. If the flow speed of the experiment (characterized by the Reynolds number) is modified the shear stress  $\tau$  of the experiment is changed, but the dimensionless wall distance  $y^+$  (including a factor  $\sqrt{\tau}$ ) remains constant, the geometrical thickness of the viscous sublayer varies with the change of the Reynolds number.

### 3.2 The complete transition turbulent-to-laminar

The minimum dissipation requirement is applied to characterize the transition of the turbulent flow experiment (including the viscous sublayer, described in chapter 3.1) to a complete laminar flow experiment by decreasing the flow speed.

The turbulent flow profile is flatter in the centre and steeper near the wall. Due to  $\tau = \text{const.}$  the dissipation of the turbulent logarithmic profile is lowest in the centre of the experiment. After the transition the final laminar profile is simply linear. The transition takes place when the turbulent dissipation in the centre is higher than the laminar dissipation at any position of the profile. That situation defines the “critical” number  $Re_{crit}$

We use three parameters according Fig. 2.

- The factor  $f = f_{min}$  as indicator of the change of the wall shear stress during transition
- The dimensionless wall distance  $y_m^+$  of the centre of the Couette flow as critical wall distance
- The critical Reynolds number of the Couette flow  $Re_{crit} = \frac{2 u_m \cdot y_m}{\frac{\mu}{\rho}}$  as minimum condition

With  $\tau$  according Eq. 8 the dimensionless wall distance  $y^+ / 8/$  becomes

$$y_m^+ = y_m \cdot \sqrt{\frac{\mu \cdot f \cdot \frac{u_m}{y_m}}{\rho}} \cdot \frac{1}{\frac{\mu}{\rho}} \quad (13)$$

and introducing the turbulent definition of  $\tau$  in Eq. 8

$$y_m^+ = y_m \cdot \sqrt{\rho \chi^2 \cdot y_m^2 \cdot \frac{1}{f^2} \cdot \left(\frac{u_m}{y_m}\right)^2} \cdot \frac{1}{\rho} \cdot \frac{1}{\frac{\mu}{\rho}} \quad (14)$$

Eq. 13 leads to

$$y_m^+ = \sqrt{f \cdot \frac{1}{2} \cdot Re_{crit}} \quad (15)$$

and Eq. 14 to

$$y_m^+ = \chi \cdot \frac{1}{2} \cdot \frac{1}{f} \cdot Re_{crit} \quad (16)$$

Additionally Eq. 12 and the logarithmic flow profile lead to

$$y_m^+ = f^2 \cdot 2,5 \quad (17)$$

The critical Reynolds number  $Re_{crit}$  characterizes the transition turbulent-to-laminar. By decreasing the velocity of the flow experiment, thereby decreasing the Reynolds number, the transition takes place at  $Re_{crit}$ .

The viscous layer near the wall must have lower dissipation than the turbulent dissipation off the wall.

According to Fig. 2 we assume

$$\frac{du}{dy}(y=0) = f \cdot \frac{u_m}{y_m}$$

and for the dissipation

$$\rho \chi^2 y_m^2 \left( \frac{du}{dy}(y=y_m) \right)^3 > \mu \left( \frac{u_m}{y_m} \right)^2 \quad (18)$$

and for the shear stress

$$\tau = \mu \cdot f \cdot \frac{u_m}{y_m} = \rho \chi^2 y_m^2 \left( \frac{du}{dy}(y_m) \right)^2 \quad (19)$$

Eq. 19 into Eq. 18 leads to

$$\frac{du}{dy}(y=y_m) > \frac{1}{f} \frac{u_m}{y_m} \quad (20)$$

and

$$\mu \cdot f \frac{u_m}{y_m} < \rho \chi^2 y_m^2 \cdot \frac{1}{f^2} \left( \frac{u_m}{y_m} \right)^2 \quad (21)$$

$$f^3 < \chi^2 \frac{y_m \cdot u_m}{\frac{\mu}{\rho}}$$

results

$$2 \cdot f^3 \cdot \frac{1}{\chi^2} < Re_{Couette,crit} \quad (22)$$

The definition of  $f_{min}$  in Eq. 22 contains two unknown variables,  $f_{min}$  and  $Re_{Couette,crit}$ . To identify both variables independently we discuss the linear-laminar profile and the turbulent logarithmic profile according to Fig. 2. Both profiles must give the same value of the velocity  $u_m$  in the centre of the Couette flow at the position  $y_m$ .

To calculate the logarithmic flow profile, we use the dimensionless logarithmic velocity distribution as a function of the dimensionless wall distance. According to the experimental literature [8] and Eq. 4a.

$$\varphi(\eta) = 2.5 \ln \eta + 5,5 \quad (23)$$

with

$$\varphi = u \cdot \frac{1}{\sqrt{\frac{\tau_0}{\rho}}} \quad (24)$$

as dimensionless so-called shear stress speed and

$$\eta = y \cdot \frac{\sqrt{\frac{\tau_0}{\rho}}}{\frac{\mu}{\rho}} \quad (25)$$

as dimensionless wall distance.

(The logarithmic function has a singularity near the wall  $u(y = 0) = -\infty$ ). The calculation is corrected by adding the dimensionless thickness of the viscous layer ( $y^+ = 2,5$ , Eq. 12) to the dimensionless wall distance.

The calculation of the turbulent flow profile with Eq. 23, the wall distance  $y_m$  calculated with Eq. 25 and the laminar value for  $u_m$  ( $y = y_m$ ) results in

$$f_{min} = 5,2 \quad (26)$$

With Eq. 26 results

$$Re_{Couette, Crit} = 1750$$

Schlichting describes /8/ experimental critical values of  $Re_{\text{Couette}} = 1500$  (that would correspond to  $f_{\min} = 4,95$ ).

### 3.3 The “forced” changeover laminar-to-turbulent

The minimum dissipation requirement is applied to describe the significant difference of the near-wall transition (chapter 3.1) and of the complete transition turbulent-to-laminar (chapter 3.2) to any transition in a flow experiment to turbulence.

The change-over laminar-to-turbulent demonstrates significant differences compared to the transition turbulent-to-laminar (chapter 3.2).

The flow experiment starts with low laminar flow rates. Increasing the flow rates it is demonstrated by experiment that the laminar flow can be maintained up to very high Reynolds numbers at least  $> 50000$  (tube flow).

Any “transition” to turbulence contradicts the minimum dissipation requirement. Consequently that “transition” does not take place.

Landau (Nobel Prize 1961) suggested two different critical Reynolds numbers for both directions of transition but was not successful “because currently there is no evidence that such cases of instability really exist” /12/.

Landau was right, there is no “instability”. Both flow forms, laminar, starting from low Reynolds numbers, and turbulent, starting from high Reynolds numbers, are stable at the same Reynolds number. Any “transition” has to be “forced” as demonstrated by experiment /13/. The experiment shows that any transition is “not triggered by the implication of disturbances” /11/. The transition can be triggered by “special features of the test section”. A critical triggering height of step-like obstacles has been quantified by Durst /11/.

The preceding chapters show that a logarithmic turbulent flow profile is a significant basis for minimum local dissipation rates at sufficient great wall distance. On the other hand the logarithmic profile is always associated with higher local flow speeds and higher gradients near the wall, thereby with higher wall shear stress, higher flow resistance, higher total dissipation of the Couette experiment. The blended effect is an increase of the wall shear stress by a minimum factor  $f$  ( $f_{\min} \cong 5$  for the Couette flow), thereby the dissipation, thereby the additional

mechanical power input into the experiment. Without that required additional power input no changeover takes place.

The minimum dissipation requirement is applied to describe the “forced” change-over. That means that at a given Reynolds number, reached by stable laminar flow, the “forced” manipulation of the profile requires a defined increase of the mechanical power input into the experiment by the factor  $f$ , given in Fig. 5. For completing the “forced” change-over the turbulent dissipation at maximum wall distance has to be lower than the original laminar dissipation. Inverting the signs in Eq. 18 to Eq. 21 leads to

$$\frac{du}{dy_t}(y = y_m) \leq \frac{1}{f} \frac{u_m}{y_m} \quad (27)$$

$$\mu \left(\frac{u_m}{y_m}\right)^2 \geq \rho \chi^2 \cdot y_m^2 \left(\frac{du}{dy}(y = y_m)\right)^3 \quad (28)$$

$$f^3 \geq \chi^2 \frac{y_m \cdot u_m}{\rho} \quad (29)$$

$$y_m^+ = f^2 \cdot 2,5 \quad (30)$$

Fig. 1 shows to velocity profiles for  $Re = 2900$  and  $Re = 34000$ . The slope of the flow profile near the wall becomes steeper with increasing Reynolds numbers. (This is also observed in the turbulent flow profiles of the tube flow and the boundary layer flow /8/).

Contrary to Chapter 3.2 we are now interested in maximum  $f$ -values.

The minimum dissipation requirement gives the answer. With

$$\tau = \text{const.}$$

and Eq. 1, 2 and 3 follows

$$\frac{du}{dy} \cong \frac{1}{y}$$

The dissipation is at its minimum at maximum conceivable  $y$ -values in the centre of the experiment at  $y = y_m$ .

Fig. 5 shows the influence of increasing Reynolds numbers on the increase of the wall shear stress given by the  $f$ -value. The  $f$ -value is calculated with Eq. 29 and the wall distance  $y_m^+$  at the centre of the flow experiment as dimensionless value with Eq. 30. That corresponds to a steeper profile near the wall, corresponding to a lower dissipation rate in the centre, compared to the original laminar flow profile.

The  $y_m^+$  values at lower Reynolds numbers ( $Re \leq 10000$ ) show that a significant part of the profile at  $y^+ < 70$  /8/ is part of the transition zone.

Re	$f_{\text{Couette}}$	$y_m^+$
1750	5,2	67,5
2900	6,15	97
4000	6,5	118
10000	9,3	215
20000	11,7	340
34000	13,1	430
60000	16,9	710

Fig. 5: f-factors of Couette flow

$\frac{\lambda_{\text{turb}}}{\lambda_{\text{lam}}}$
8,1
13,2
18,6

Fig. 5b:  $\frac{\lambda_{\text{turb}}}{\lambda_{\text{lam}}}$  pipe flow

With increasing Re-numbers the turbulent flow profile near the wall becomes steeper, as shown with the increasing f-factor in Fig. 5.

Experimental values for the Couette flow are not available. One can compare some results at higher Reynolds numbers  $Re > 30000$  with experimental results for the tube flow. By comparing the laminar flow resistance ( $\lambda_{\text{lam}}$ -value of the Hagen-Poiseuille formula /8/) with the experimental turbulent formula ( $\lambda_{\text{turb}}$ -value of the Blasius formula /8/) one gets an indication of the change of the wall shear-stress between laminar and turbulent profile. In Fig. 5b  $\frac{\lambda_{\text{turb}}}{\lambda_{\text{lam}}}$  can be compared with the f-value. At  $Re > 30000$  these values are  $< 10\%$  different from the f values in Fig. 5. At lower Reynolds numbers there is a factor 2.

To “force” the change-over an increase of the mechanical power input by a factor 5-17 is required. That consequence is compatible with the statement of Oertel jr. /18/, that “turbulence has nothing to do with instability”.

### 3.4 Results and consequences

The experimental results and the application of the minimum dissipation theorem give the following consequences for the Couette flow.

#### 1. Consequence

The Couette flow experiment shows three different flow mechanisms.

- The turbulence, described by the empirical logarithmic “law of the wall” as non-local mechanism, limited above  $y^+ > 70$  (theory  $y^+ > 67,5$ ).
- The local Navier-Stokes mechanism with the linear Newton-Stoke’s friction, limited below a dimensionless wall distance  $y^+ < 2,5$  (experiment  $< 2$ ).
- The transition mechanism, not known in detail.

#### 2. Consequence

Experiment and theory show three different types of transition.

- The continuous co-existence of laminar and turbulent flow above the laminar sublayer near the wall.
- The turbulent-to-laminar transition of the complete flow at  $Re_{crit}$
- The “forced” change-over laminar-to-turbulent, after increasing the input of mechanical power by a factor 5-17. Without increasing that input laminar and turbulent flow are stable at the same elevated Re-numbers and no transition takes place.

#### 3. Consequence

The generalised statements that the dissipation of turbulent flow is maximum (Malkus, Busse /6/) or is minimum (Klimontovich /7/) do both not comply with experiment and theory. In Chapter 2.1 the near-wall laminar, linear flow has a lower dissipation rate than the turbulent logarithmic flow at higher wall distance (otherwise laminar flow would not exist). At sufficient high wall distance, the turbulent dissipation rate is lower than the laminar dissipation rate (otherwise turbulent flow would not exist).

#### 4. Consequence

Unique to the Couette flow the shear stress is

$$\tau = \text{const.}$$

and the dissipation

$$\dot{E} = \tau \cdot \frac{du}{dy}$$

Dissipation and  $\frac{du}{dy}$  becomes smaller with increasing wall distance. The s-shaped turbulent flow profile (Fig. 1) and both conditions do not comply with constant definition of the Newton-Stokes viscosity of the Navier-Stokes equations.

#### 4. General conditions for turbulence, “ $\mu_{\text{turb}}$ ” $\geq 27 \mu$

The preceding results are based on one theoretical element, the minimum dissipation theorem, applied to the Couette flow.

The logarithmic flow profile (law-of-the-wall) is very important, but is only based on a hypothesis (Prandtl, v. Kármán) fitted to the experiment. It is used as a formula for experimental results. The advantage of using empirical and experimental results is the simplicity of the discussion. The disadvantage is a limited theoretical basis.

Experiment and theory show the logarithmic “law-of-the-wall” for

- turbulent flow forms
- at high wall distance  $y^+ > 67,5$
- at wall distance  $< 0,3 \cdot y_m$  (pipe experiment) /21/

For the linear laminar zone near the wall

$$\frac{du}{dy}(y = 0) = f \frac{u_m}{y_m}$$

with  $f \geq 5,2$

$$\geq 5,2 \cdot \frac{u_m}{y_m}$$

According Eq. 20 for the turbulent zone near the centre  $y = y_m$

$$\frac{du}{dy}(y = y_m) = \frac{1}{f} \frac{u_m}{y_m}$$

With the result

$$\frac{du}{dy}(y = y_m) = \frac{1}{f^2} \frac{du}{dy}(y = 0)$$

with  $f \approx 5,2$

$$\leq \frac{1}{27} \frac{du}{dy}(y = 0)$$

With the important and unique feature  $\tau = \text{const.}$  of the Couette flow

$$\tau(y = 0) = \tau(y = y_m)$$

$$\mu \cdot \frac{du}{dy}(y = 0) = \mu_{turb} \cdot \frac{du}{dy}(y = y_m)$$

or

$$\frac{\mu_{turb}}{\mu} \geq 27$$

The same result is described in /15/ with a different approach, the minimum dissipation theorem implementing a non-local (corpuscular) model for turbulent structures and using Taylor's formula for isotropic turbulent fluctuations. The approach is described by Drescher in /15/, resulting in a criterion for the existence of turbulence, defined by a minimum condition of the "apparent" turbulent viscosity " $\mu_{turb}$ "  $\geq 27 \mu$

An empirical result is given by  $\tau = const.$  (Couette flow),

$$\tau \sim y^2 \left( \frac{du}{dy} \right)^2 \text{ (logarithmic flow profile, Prandtl's hypothesis), at } 60 < y^+ < y_m^+ \text{ /8/}$$

An analytical result is given by

$$\tau \sim \frac{du}{dy} \text{ (Navier-Stokes Eq., Newton-Stokes viscosity), at } y^+ < 2,5$$

For the Couette flow  $\tau = const.$  is mandatory, and the minimum dissipation requires  $\frac{du}{dy}$  decreasing monotonously above  $y^+ > 2,5$ .

## 5. Limitations of the logarithmic “law-of-the-wall”

The logarithmic shape of the turbulent flow profile has been admired remarkably as an important and classical result. Marusic emphasizes: “The beauty of this classical result is its simplicity particularly given the complexity of the multi-scale non-linear problem at hand” /14/. Schlichting describes the “law-of-the-wall” (curve 3 in Fig. 3) as “excellent compliance” /8/.

We shall review the enthusiasm of Marusic and Schlichting. At low Re-numbers the experimental data in Fig. 3 do not comply with Eq. 4a below  $y^+ \cong 50$  (Fig. 4 uses Eq. 4b which is 10 % lower). The logarithmic law (curve 3 in Fig. 3, straight line in Fig. 4) includes a singularity near the wall. At  $y^+ = 0$  the value is  $\varphi(0) = -\infty$ . At  $y^+ = 1$  the value is only defined by the arbitrary integration constant (5,5 in Eq. 4a; 5,17 in Eq. 4b). There are further restrictions of the logarithmic law for the centre of the pipe flow and greater wall distances. M. Platzer has summarized and quantified these effects and described the possible corrections /19/. Restrictions are mentioned by K. Wieghardt /20/ and St. Pope /21/.

K. Wieghardt summarizes experimental and theoretical results in Fig. 6 and states that the logarithmic law-of-the-wall is “valid nearly in the complete pipe area”, but not “near the wall and in the pipe centre” /20/. St. Pope doubts the logarithmic law above  $0,3 \cdot y_m$  /21/. F. Durst measured the differences at low Reynolds numbers  $Re < 9800$  /9/ (see Fig. 4).

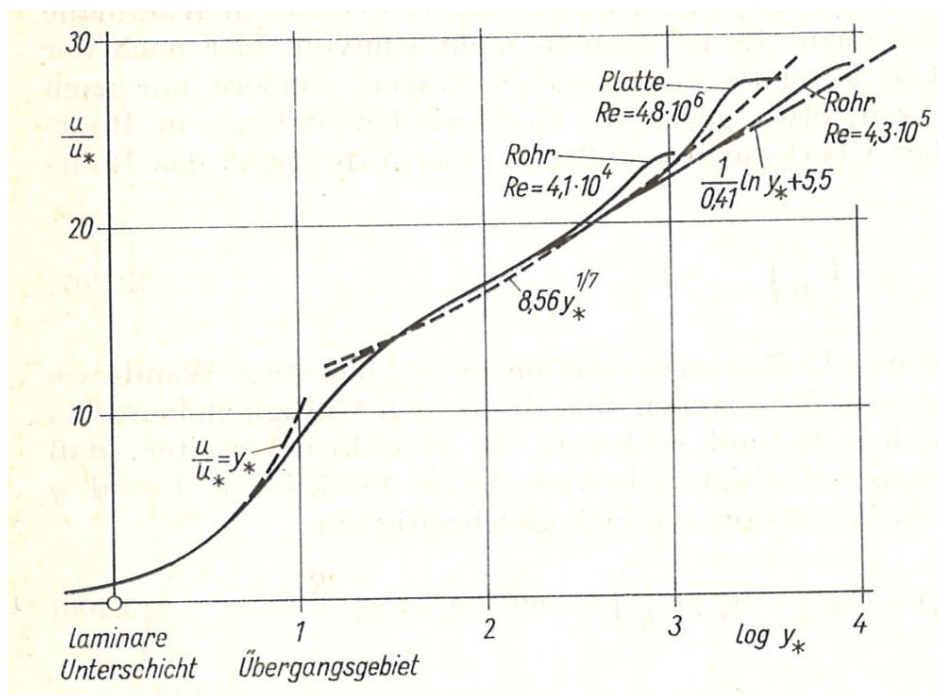


Fig. 6: Turbulent flow profiles, K. Wieghardt /20/

The reasons for the deviations of the logarithmic law are not discussed in detail. Important is that the formula is completely “local”, the derivation of Prandtl’s mixing length hypothesis is “non-local”.

One wrong result is the finite gradient of the logarithmic formula at the centre of the pipe. That includes a kink of the profile at the centre.

The non-local character of turbulence is a second important feature to characterize turbulence. The following chapters focus on that feature by a “corpuscular” model of the fluid behaviour. The model confirms important parts of the logarithmic law but avoids the criticised result near the centre of the pipe.

## 6. An analytical model: non-local character, logarithmic flow profile, v. Kármán constant, Prandtl's mixing length

It is interesting to compare a “corpuscular” model for turbulent flow behaviour with the empirical results of Prandtl's and v. Kármán's “universal law of the wall”.

We consider plane Couette flow, as shown in Fig. 7. Contrary to laminar Couette flow the flow profile is not linear but S-shaped and is indicative of later results. We consider a volume with a dimension  $D$  at a sufficient distance from the walls. The dimension  $D$  is macroscopic but unknown in detail.

We assume that momentum exchange takes place in this volume element and that any dissipation takes place with delay.

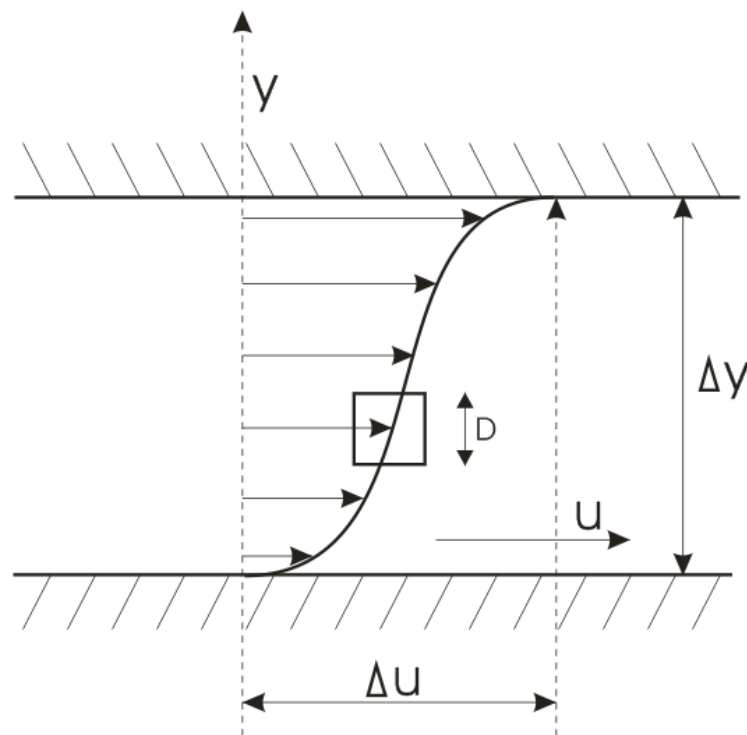


Fig. 7: Plane Couette flow

The origin of the coordinates is assumed to be at the centre of the D-element (Fig. 6). With a linear profile,  $\frac{du}{dy} = \text{constant}$ , the kinetic energy  $E_{Kin}$  of all the mass points of the D-element is

$$E_{Kin} = D^2 \int_{-D/2}^{D/2} \frac{1}{2} \rho \left( \frac{du}{dy} y \right)^2 dy = \frac{1}{24} \rho \left( \frac{du}{dy} \right)^2 D^5 \quad (31)$$

After momentum exchange, all the mass points may possess equal kinetic energy. Thus, the resulting mean value of the velocity given by  $|V_{qu}|$  is

$$\frac{1}{2} \rho D^3 V_{qu}^2 = \frac{1}{24} \rho \left( \frac{du}{dy} \right)^2 D^5 \quad (32)$$

$$|V_{qu}| = \frac{1}{\sqrt{12}} \frac{du}{dy} D$$

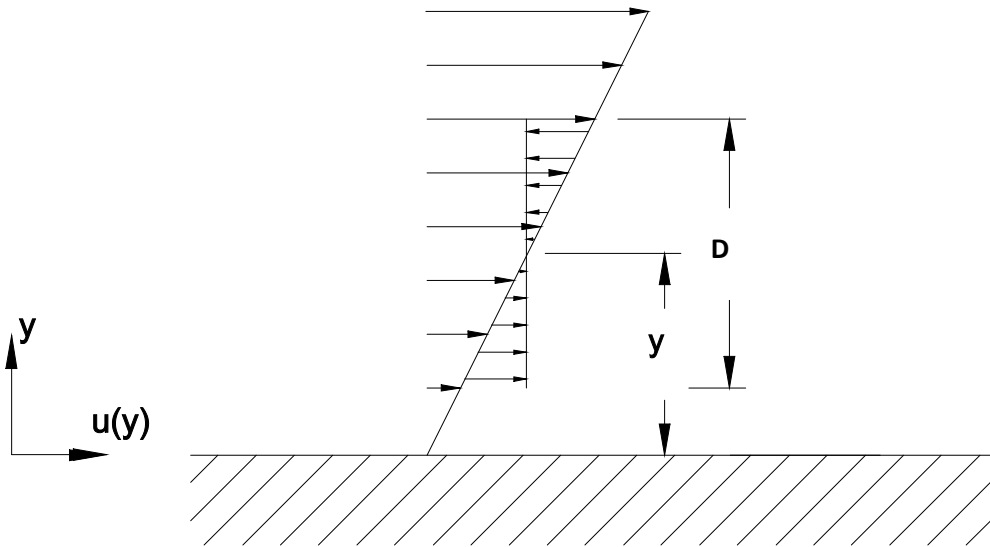


Fig. 8: Momentum exchange within the D-element

In this way, an averaged total momentum of the upper and lower half spaces is adapted.

We now determine the momentum exchange  $\Delta p$  on the surface  $y = \text{constant}$  in the centre of the D-element as a measure of the “apparent” shear stress  $\tau$ .

Further calculation leads to the apparent “shear stress”  $\tau$

$$\tau = \frac{\Delta p}{\Delta T} \quad (33)$$

$$\tau = \frac{1}{6\sqrt{3}} \rho \left( \frac{du}{dy} \right)^2 D^2 \quad /15/$$

An equivalent calculation is given in /15/. We verify the result by adopting the “analogy to the kinetic theory of gases” described in Prandtl’s mixing length hypothesis /8/. According to the kinetic theory of gases the viscosity is

$$\mu = \frac{1}{3} \rho l \bar{c} \quad (34)$$

where  $\rho$  is the density,  $l$  the mean free distance, and  $\bar{c}$  the mean velocity of gas molecules.

Replacing the mean free distance  $l$  with  $D$  and the mean molecular velocity  $\bar{c}$  with  $V_{qu}$ , the apparent “viscosity”  $\mu_t$  is given by

$$\begin{aligned} \mu_t &= \frac{1}{3} \rho D V_{qu} \\ &= \frac{1}{6\sqrt{3}} \rho \frac{du}{dy} D^2 \end{aligned} \quad (35)$$

which confirms the mentioned result in Eq. 33.

A question arises on the possible dimension of  $D$ . For this question, the condition of minimum dissipation gives a surprising result.

The local dissipation  $\dot{E}$  can be expressed as

$$\dot{E} = \tau \frac{du}{dy}$$

or, with  $\tau$  according to Eq. 33,

$$\dot{E} = \sim \left( \frac{du}{dy} \right)^3 D^2$$

For any Couette flow profile, the shear stress is constant

$$\tau = \sim D^2 \left( \frac{du}{dy} \right)^2 = \text{const.} \quad (36)$$

or

$$\frac{du}{dy} \sim \frac{1}{D} \quad (37)$$

Thus,

$$\dot{E} \sim \frac{1}{D} \quad (38)$$

The dissipation decreases as D increases. For the dissipation to be at its minimum, D has to assume a maximum value – this characterizes the dissipation  $\dot{E}$  as “non-local”.

The maximum possible D-values are limited by the fact that the D-volume must not approach the walls. From the condition of continuity and the assumed incompressibility of the fluid near the wall, it follows that the volume is displaced by transverse flow at a velocity that increases as the distance from the wall decreases and D increases. Excessive dimensions and close proximity to the wall would contradict the definition of the D-element (undisturbed momentum exchange).

Proximity to the wall is a limiting factor for a maximum value of D. The approach below is chosen, where

$$D = \alpha y \quad y = \text{wall distance} \quad (39)$$

The approach with a scaling factor  $\alpha$

$$\alpha = \frac{4}{3}$$

provides an idea of the maximum conceivable dimension of a D-volume with momentum exchange that is still “undisturbed” despite its proximity to the wall (Fig. 7).

Eq. 33, Eq. 38 and Eq. 39 lead to a logarithmic flow profile. The shear stress  $\tau$  is

$$\begin{aligned}\tau &= \frac{16}{9} \cdot \frac{1}{6\sqrt{3}} \rho \cdot y^2 \left(\frac{du}{dy}\right)^2 \\ &= 0,171 \rho \cdot y^2 \left(\frac{du}{dy}\right)^2\end{aligned}\tag{40}$$

Comparison with Eq. 3 gives a value

$$\chi = 0,415$$

to be compared with the empirical v. Kármán constant  $\chi$ .

The conclusion that the characteristic dimensions of turbulence assume maximum values results in a change in perspective: turbulence is not the result of “instable” laminar motion but a stable condition or, as argued by Klimontovich /7/, focusing the minimum condition, “turbulent flow has a greater degree of order than laminar flow”. Marusic et al. /14/ mentioned that there are “many unanswered questions in respect of very large scale motions (VLSMs)” or “superstructures” /14/.

The question then arises of how far this can be observed in the free atmosphere. The spatial extent and the temporal course of the occurring flow events are of particular interest. We expect turbulence elements >100 m and exchange times of several minutes.

For such an observation, the visible part of cooling tower plumes can be used. Such a plume is saturated with water vapour and becomes visible – similar to a cloud – through condensed water droplets. At a certain distance from the source, it can usually be observed that the plume “dissolves”. This “dissolution” is mainly caused by turbulent mass and heat exchange. Large-scale exchange processes must therefore become visible on large structures of the plume image. The area where the plume has dissolved and only a few shreds remain is particularly interesting. Some of the distances between them show a very distinctive scaling (Fig. 9).



Fig. 9: Weisweiler power plant, 12/26/2009, 9.26 Uhr (1 min. time difference),  
temperature 4 °C, wind 230 °/7-10 m/s

Prandtl's mixing length hypothesis is an important step in explaining turbulent flow behaviour. The hypothesis does not utilize the Navier-Stokes equations.

Prandtl assumes that in turbulent flow, packets of fluid have independent motion and move both longitudinally and laterally over an average distance  $l$ , under conservation of their momentum. The resulting fluctuations are explained by fluid packets of different velocities encountering each other. Prandtl describes the mixing length by adopting an "analogy to the kinetic theory of gases" [8]. A further result of Prandtl and v. Kármán is the logarithmic shape of the turbulent flow profile. This has been admired as an important and classic result.

The turbulent shear stress  $\tau$  and the mixing length  $l$  are calculated as

$$\tau = \rho l^2 \left( \frac{du}{dy} \right)^2 \quad (41)$$

with

$$l = \chi \cdot y$$

$$\chi = \text{v. Kármán constant}$$

$$\approx 0,4$$

$$\tau \approx \rho \cdot 0,16 \cdot y^2 \cdot \left( \frac{du}{dy} \right)^2$$

Prandtl's theory makes no statement on the size and form of the fluid packets. The dimension of the mixing length  $l$  is determined empirically from the flow profile of the experiment.

Some arguments in Prandtl's mixing length hypotheses are noteworthy.

- The mixing length is defined as a locus function of the wall distance. This is questionable because every location of the flow profile is reached and influenced by mixing lengths of different sizes and from all directions.
- The mixing length gives no indication of the thickness of the laminar boundary layer near the wall and of the transition to turbulence.

- The definition of the mixing length is an exclusively empirical operand rather than a phenomenological measure for the range of turbulent mixing motion. Prandtl's formulation lacks a factor of 1/3 if one considers  $l$  as the physical measure for a "range" of convective momentum exchange (this factor of 1/3 is not important for the hypothesis because  $l$  is determined empirically) /12/.

For a comparison, we substitute  $l = 0,4 y$  ( $y =$  wall distance) in Eq. 40 and  $D = \frac{4}{3}y$  in Eq. 33.

As a result,

Prandtl's and v. Kármán's empirical Eq. 41 becomes

$$\tau = \rho \cdot 0,16 \cdot y^2 \left( \frac{du}{dy} \right)^2 \text{ near the wall}$$

compared with Eq. 40

$$\tau = \rho \cdot 0,171 \cdot y^2 \left( \frac{du}{dy} \right)^2 \text{ for Couette flow}$$

Both equations can be compared despite different origin and background.

## 7. Numerical calculations

### 7.1 A 1-dimensional equation for a turbulent profile

The previous model assumptions describe the momentum exchange while maintaining the energy balance in a volume element  $D^3$ . We apply these results to calculate the averaged flow profile in a shear flow.

Fig. 7 shows the relations. To each wall distance  $y$  there is a volume element of the dimension  $D(y)$ , in which a momentum exchange takes place with a defined frequency. This exchange leads to superimposed transverse flows, through which partial volumes are transported between  $y + \frac{D}{2}$  and  $y - \frac{D}{2}$  (the boundaries of the D-element) transversely to the main flow direction. Mathematically, this results in an “acceleration” or a “delay” to the right or left of the main flow.

Integration over all  $y$ , to which this range relationship applies, results in the resulting total acceleration, which is zero for the mean flow values in the stationary state. We determine the frequency of the momentum exchange in one of the many D-elements to be integrated. The average flow velocity is given by  $|V_{qu}|$  according to Eq. 32.

We consider the momentum exchange in the D-element to be complete when D is “crossed” with this velocity  $|V_{qu}|$ . The “time” required for this is therefore,

$$\frac{D}{|V_{qu}|} \sim \frac{1}{\frac{du}{dy}}$$

The frequency of the momentum exchange is the reciprocal of this

$$\sim \frac{du}{dy}$$

With the integration limits  $y_{min}$  and  $y_{max}$  according Fig. 9 we obtain the following equation.

$$\frac{du}{dy}(y) \sim \frac{1}{y_{max}-y_{min}} \left[ \int_{y_{min}}^{y_{max}} \left( \overline{u(\tilde{y})} - u(y) \right) \frac{d\overline{u}}{dy}(\tilde{y}) d\tilde{y} \right] \quad (42)$$

$$= 0$$

for stable conditions.

The values  $\overline{u(\tilde{y})}$  and  $\overline{\frac{du}{dy}(\tilde{y})}$  in the integral of Eq. 42 are not to be seen as point values, but as average values over the range of the D-element around  $\tilde{y}$  and are therefore marked.

The integration limits  $y_{max}$  and  $y_{min}$  result from  $D = \frac{4}{3}y$ , for the area near the wall with

$$y_{max} = 3y$$

$$y_{min} = \frac{3}{5}y$$

For the integration limits defined in this way, it applies that the D elements around  $y_{min}$  resp.  $y_{max}$  just reach the point  $y$ .

$$y_{max} - \frac{1}{2}D(y_{max}) = y$$

$$y_{min} + \frac{1}{2}D(y_{min}) = y$$

Fig. 10 shows the geometric relationship.

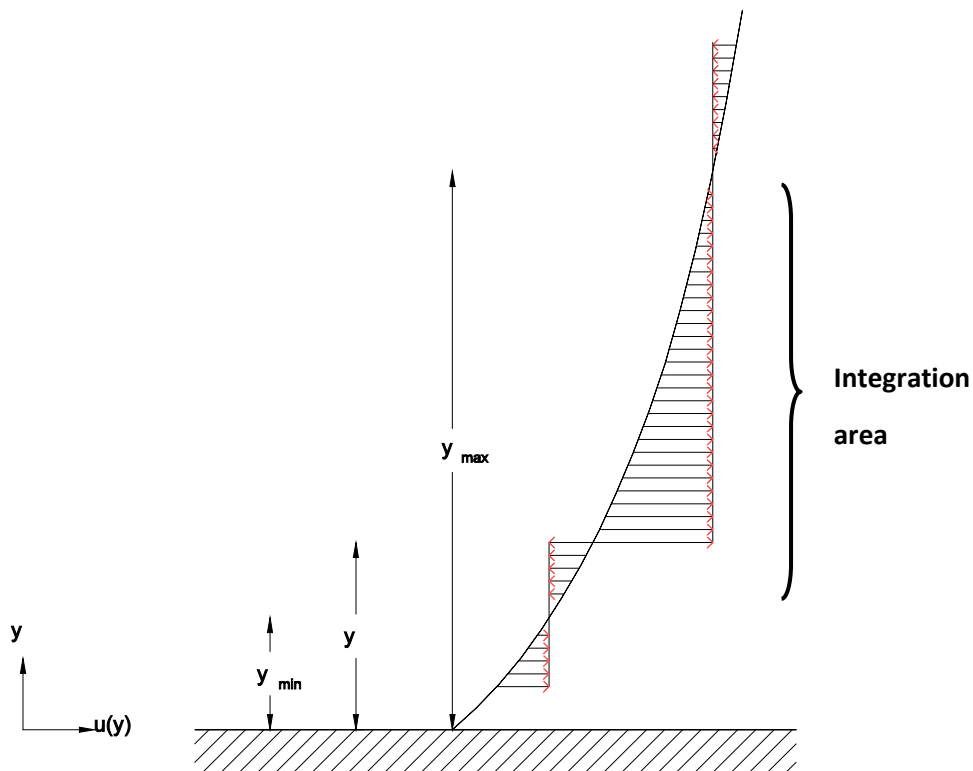


Fig. 10: Integration according to Eq. 42

The integration limits defined in this way correspond to the maximum property, but do not necessarily fulfil the minimum property. This applies in particular in the vicinity of the wall, i.e. for small  $y$  and thus small  $y_{min}$ . We therefore designate with  $y_-$  the smallest wall distance for which the minimum condition

$$"\mu_{turb}(y_-)" \geq 27\mu$$

still applies. An integration of Eq. 42 in the direction of the wall is thus physically permissible for

$$\begin{aligned} y_{min} &\geq y_- - \frac{1}{2}D(y) \\ &\geq \frac{1}{3}y_- \end{aligned} \tag{43}$$

The turbulent flow profile is calculated according to the integral Eq. 42 under auxiliary conditions for the maximum and minimum values of the integration limits.

Parallel to this and especially outside the constraints, Newton's equation applies.

## 7.2 Numerical examples for Couette and pipe flow

Eq. 42 can only be solved analytically under simplified assumptions. We take a numerical approach, the flow profile  $u(y)$  over the cross-section  $y$  is divided into a staircase function according to Fig. 11.

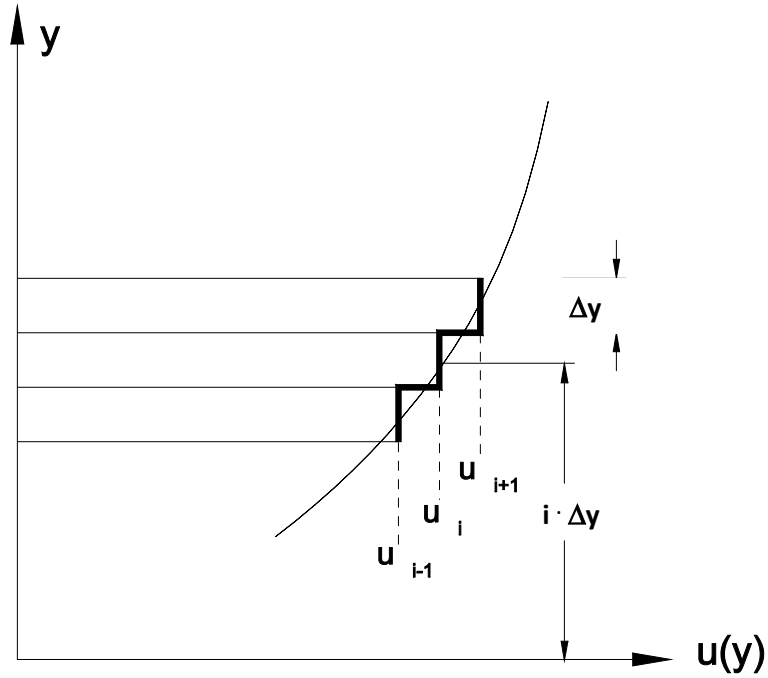


Fig. 11: Stair function for profile calculation

The step width is  $\Delta y$ , the respective step value  $u_i$  corresponds to the average value of  $u$  in the interval  $\Delta y$  around the coordinate value  $y = i \Delta y$ .

By analogous application of Eq. 42, each  $u_i$  in each iteration step is changed by one  $\Delta u_i$  according to the following calculation rule.

$$\Delta u_i \sim \frac{1}{(K_{max} - K_{min})} \sum_{K=K_{min}}^{K_{max}} (\overline{u_K} - u_i) \frac{\overline{\Delta u_K}}{\Delta y}$$

if " $\mu_{turb}$ "  $< 27\mu$

$$\sim \frac{\mu}{\rho} \left( \frac{u_{i+1} - u_i}{\Delta y} - \frac{u_i - u_{i-1}}{\Delta y} \right) \frac{1}{\Delta y}$$

+ constant

(44)

$\overline{u_K}$  and  $\frac{\overline{\Delta u_K}}{\Delta y}$  are analogous to Eq. 42 numerical average values over the range  $K \cdot \Delta y \pm \frac{1}{2} D(K\Delta y)$ .

The summation in the first line is made for those  $u_K$  for which the turbulence conditions from Chapter 4 are fulfilled. The summation interval results from the definition of  $K_{min}$  and  $K_{max}$  according to the definition of Eq. 42 with the constraints  $K_{min}$  and  $K_{max}$ . mentioned.

The second line considers the Newtonian laminar friction.

The step size  $\Delta u_i$  is limited by a selectable factor (not specified in the above calculation rule).

Furthermore, the calculated values  $u_i + \Delta u_i$  must be normalized to the total flow rate  $\sum u_i = \text{const.}$  after each calculation run (except for the Couette flow). For this purpose, the quantity "constant" in the third line is used, which is determined after each calculation and added to the newly set values  $u_i$  ("constant" corresponds to the element  $-\frac{dp}{dx}$ ). The normalization is therefore part of the calculation (not with the Couette flow, since here  $\frac{dp}{dx} = 0$ ).

The numerical results in Fig. 12 show the recalculation of the two empirical turbulent Couette profiles in Fig. 1.

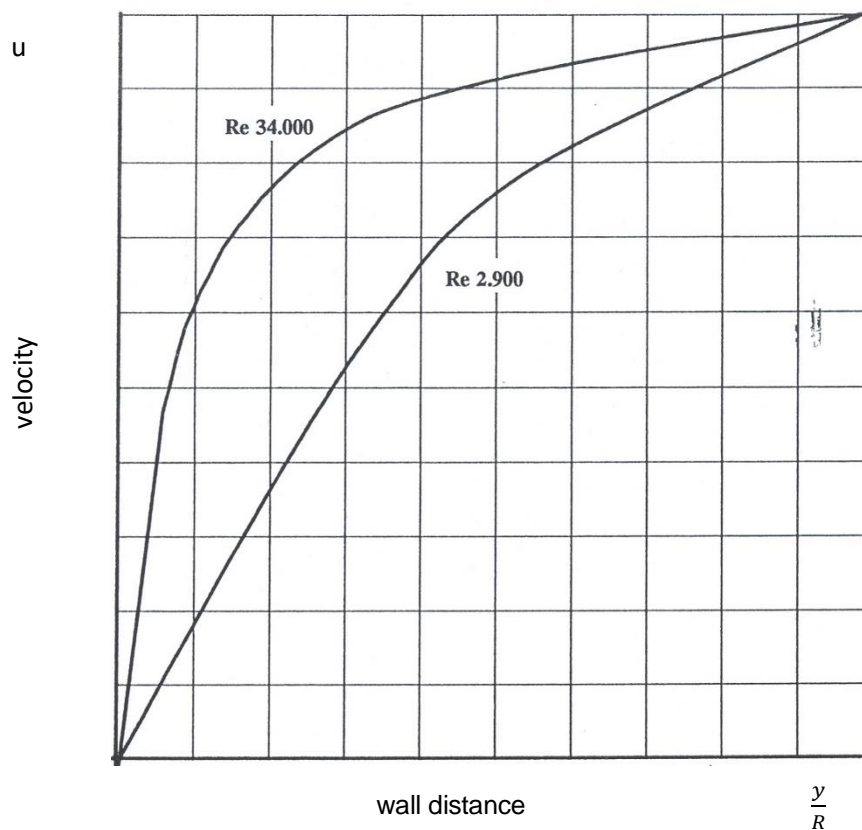


Fig. 12: Numerical calculations for the turbulent Couette flow

Fig. 13 shows the pipe/channel calculations for the Reynolds numbers 4000, 25000,  $10^5$  and  $10^6$ . The iteration with 100 support points starts with a laminar profile (linear Couette profile, Hagen-Poiseuille pipe profile) and requires 500-1000 steps. For the values in the area of the first support point, limitations of the stability apply with large Re numbers. All curves show finite gradients near the wall.

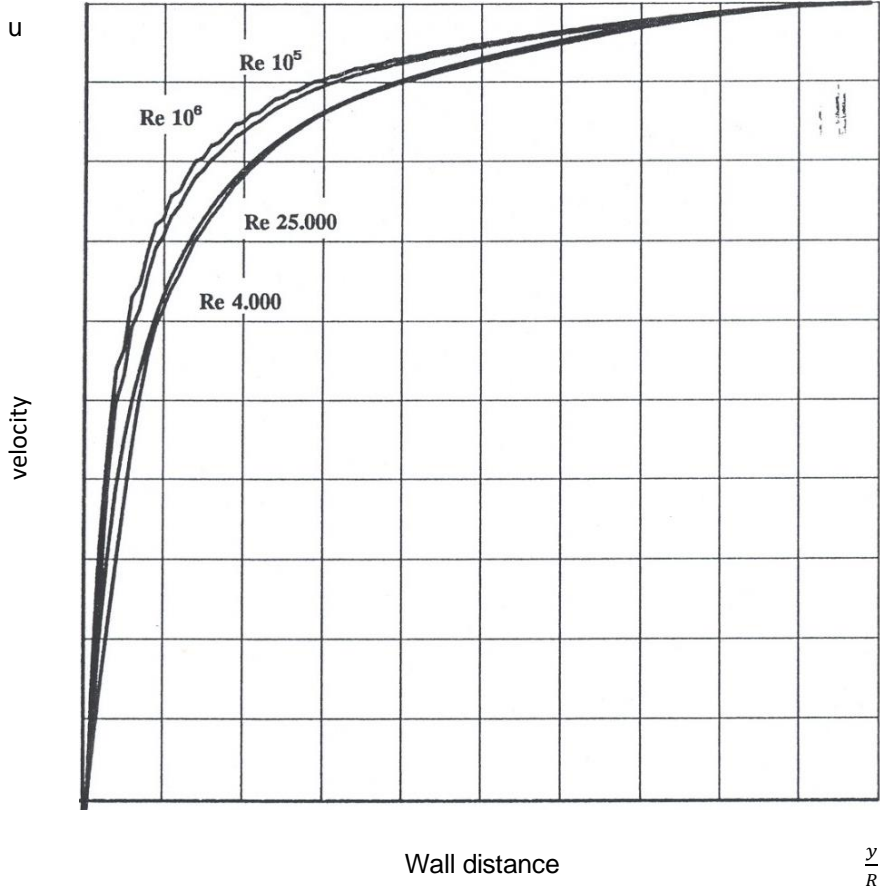


Fig. 13: Numerical calculations for the pipe flow

Infinitely high gradients near the wall are not applicable there, but are often found in the literature. The gradient is clearly determined by the flow resistance values for the pipe flow.

## 8. Summary

The theorem of minimum entropy production/dissipation of the thermodynamics of irreversible processes is applied to experimental and theoretical results of the Couette flow. The physical principle indicates that every form of transition or change can be identified by a variation of the dissipation rate.

The thickness of the viscous sublayer, of the transition zone, the near wall gradient and the critical Reynolds number are calculated based on the minimum dissipation criterion.

Turbulence includes an increase of flow resistance thereby of the dissipation. At the first glance that contradicts the minimum dissipation requirement. The direct consequence is the logarithmic flow profile, leading to lower local dissipation rates at sufficient high wall distances, in spite of the increasing total flow resistance.

The consequence of the logarithmic profile is a steeper flow profile near the wall, causing a higher local dissipation near the wall, and a flatter profile, causing a lower dissipation off the wall. The blended effect of higher near wall dissipation and lower dissipation at sufficient distance of the wall requires a local position at which the minimum condition is fulfilled. The critical Reynolds number is explained by that.

With transition to turbulence a sudden increase of the wall shear stress by a factor  $f > 5$  is observed. That requires an increase of the input of mechanical energy into the experiment by that factor. Without that no transition takes place, the laminar flow remains stable up to elevated Reynolds numbers. That confirms experimental results of F. Durst and indicates that the transition to turbulence is “not triggered by the amplification of disturbances” /11/ but has to be “forced” /13/. H. Oertel jr. /18/ mentions the discussion that “turbulence has nothing to do with instability”.

The “local” definition of the Newton-Stokes viscosity does not comply with the “non-local” character of turbulence. This question is discussed by Ph. Spalart as “fundamental paradox” between the local character of the Partial Differential Equations and the non-local character of turbulence /16/. Mishra describes a “lack of amenability to single-point turbulence modelling” /17/.

The logarithmic “law-of-the-wall” does not comply near the wall due to a mathematical singularity and near the centre of the pipe flow due to a finite gradient at  $y = y_m$ .

A “corpuscular” (non-local) model is discussed. Based on the condition of minimum dissipation maximum turbulent dimensions result and a calculated value  $\chi = 0,415$  of the v. Kármán constant. Numerical calculations respecting non-local features are presented.

The s-shaped turbulent Couette profile and the constant Couette shear stress are not described by the Navier-Stokes equations.

## **9. Acknowledgments**

The author thanks F. Durst, Erlangen, and U. Nehring, Göttingen for important remarks and theoretical and experimental information, concerning the keywords “nonlocal physical nature” and “forced transition” of turbulence.

## Literature

- /1/ /1b/ I. Prigogine, Introduction to thermodynamics of irreversible processes, 3. Auflage, 1967  
I. Prigogine, Zeit, Struktur und Fluktuationen (Nobel-lecture), Université Libre de Bruxelles, The University of Texas at Austin (USA), Angew. Chem. 90, 704-715 (1978)
- /2/ Brockhaus Enzyklopädie, 17. Auflage, Bd. 15, 1972, 137
- /3/ Encyclopaedia Britannica, 15 Edition, Vol. 28, 641-645
- /4/ L. D. Landau, E.M. Lifschütz, Lehrbuch der theoretischen Physik, Bd. 1, Mechanik, Berlin 1967
- /5/ A. Budó, Theoretische Mechanik, Berlin 1965
- /6/ W.V.R. Malkus, Outline of a theory of turbulent shear flow, J. Fluid Mech. 1, (1956) 521  
F. H. Busse, Bounds for turbulent shear flow, J. Fluid Mech., vol. 41, part 1, (1970), 219-240
- /7/ Yu. L. Klimontovich, Kh. Engel-Kherbert, Average steady Couette and Poiseuille turbulent flows in an incompressible fluid, Sov. Phys. Tech. Phys. 29 (3), March 1984  
Yu. L. Klimontovich, Entropy and entropy production in laminar and turbulent flows, Sov. Tech. Phys. Lett. 10 (1), January 1984
- /8/ H. Schlichting, Grenzschichttheorie, 8. Auflage, Braun, Karlsruhe 1982, 600-601, 603, 619
- /9/ F. Durst, M. Fischer, J. Jovanovic, H. Kikura, Methods to set up and investigate low Reynolds number, fully developed turbulent plane channel flows, Lehrstuhl für Strömungsmechanik, Universität Erlangen-Nürnberg, 1998.
- /10/ H.P. Drescher, Turbulence, the Millennium Stokes Problem, Jülich 2018  
[www.turbulence-problem.de](http://www.turbulence-problem.de)

- /11/ F. Durst, K. Haddad, Ü. Erteunc, A pipe flow test section to demonstrate the causes of laminar-to-turbulent transition, July 2019
- /12/ L. D. Landau, E.M. Lifschitz, Lehrbuch der theoretischen Physik, Bd. 6, Hydrodynamik, Berlin 1966, 120
- /13/ F. Durst, B. Ünsal, Forced laminar-to-turbulent transition of pipe flows, J. Fluid Mech. (2006) vol. 560, pp. 449-464
- /14/ I. Marusic, B. J. McKeon, P.A. Monkewitz, H. M. Nagib, A.J. Smits, K.R. Sreenivasan, Wall-bounded turbulent flows at high Reynolds numbers: Recent advances and key issues, Physics of Fluids 22 (2010)
- /15/ H.P. Drescher, The irreversible thermodynamic's theorem of minimum entropy production applied to laminar and turbulent Couette flow, Jülich, 2018, [https://www.budi.de/files/downloads/minimum\\_entropy\\_production.pdf](https://www.budi.de/files/downloads/minimum_entropy_production.pdf)
- /16/ Ph. Spalart, Philosophies and fallacies in turbulence modeling, Seattle USA, Progress in Aerospace Sciences 74 (2015) 1-15
- /17/ Aashwin Ananda Mishra, Sharath Girimaji, Linear analysis of non-local physics in homogeneous turbulent flows, Phys. Fluids 31, 035102 (2019)
- /18/ Prandtl-Führer durch die Strömungslehre, 13. Auflage, Springer, 2012, (ed. by H. Oertel jr.)
- /19/ M. Platzer, Pebble Beach, CA, USA, Personal summary, 2020
- /20/ K. Wieghardt, Theoretische Strömungslehre, Teubner, 1965
- /21/ St. Pope, Turbulent flow, Cambridge University Press, 2000

## Special parameters

$\tau$	shear stress
$\dot{E}$	local dissipation
$f$	ratio turbulent/laminar of $\tau$
$\mu$	viscosity
$\mu_{turb}$	apparent “turbulent” viscosity
$\rho$	density
$\chi$	v. Kármán constant
$l$	Prandtl’s mixing length
$u$	speed
$\bar{u}$	average speed
$u'$	speed fluctuation
$u_x$	so-called shear stress speed (dimensionless) ( $= \varphi$ )
$y$	wall distance
$y^+$	so-called dimensionless wall distance ( $= \eta$ )

## Data Availability Statement

The data that supports the findings of this study are available within the article (and its supplementary material).